



ACADEMIC  
PRESS

Available online at [www.sciencedirect.com](http://www.sciencedirect.com)

SCIENCE @ DIRECT®

Journal of Sound and Vibration 268 (2003) 103–113

JOURNAL OF  
SOUND AND  
VIBRATION

[www.elsevier.com/locate/jsvi](http://www.elsevier.com/locate/jsvi)

# Experimental analysis of a high-speed railway bridge under Thalys trains

H. Xia<sup>a</sup>, G. De Roeck<sup>b,\*</sup>, N. Zhang<sup>a</sup>, J. Maeck<sup>a</sup>

<sup>a</sup> *School of Civil Engineering and Architecture, Northern Jiaotong University, Beijing 100044, China*

<sup>b</sup> *Department of Civil Engineering, Catholic University of Leuven, Heverlee B-3001, Belgium*

Received 28 June 2002; accepted 5 November 2002

---

## Abstract

In this paper dynamic experiments on the Antoing Bridge located on the high-speed railway line between Paris and Brussels are reported. The experiments were co-operatively carried out by the Northern Jiaotong University from China, the Catholic University of Leuven, the Free University of Brussels and the Belgium Railway Company NMBS-SNCB from Belgium. The bridge is composed of multi-span simply supported PC girders with spans of 50 m and U-shaped sections. The loads are the high-speed Thalys trains with articulated vehicles. The speeds of the Thalys trains were between 265 and 310 km/h. In the experiments, the dynamic responses of the bridge such as the deflections, the accelerations and the strains that were measured by a laser velocity displacement transducer accelerometers and strain gauges, respectively. Many useful results have been obtained from the analysis of the recorded data. The tests and the measured results can be a reference for the study and the design of high-speed railway bridges.

© 2003 Elsevier Ltd. All rights reserved.

---

## 1. Introduction

To meet the needs of passenger transportation, more and more high-speed railway lines are being constructed in the world. In China, the first Special Passenger Railway with a train speed of 200 km/h and a high-speed experimental section of more than 300 km/h has been built, and the high-speed railway line of Beijing–Shanghai is under planning. Under the loads of high-speed trains, the bridges are subjected to high impacts. During the design of the Special Passenger Railway, the Ministry of Railways of China organized the Academy of Railway Sciences and several universities to study the dynamic characteristics of high-speed railway bridges through

---

\*Corresponding author. Department of Burgerlijke Bouwkunde, Katholieke Universiteit Leuven, Kasteelpark Arenberg 40, Heverlee B-3001, Belgium. Tel.: +32-16321666; fax: +32-1321988.

*E-mail address:* [guido.deroeck@bwk.kuleuven.ac.be](mailto:guido.deroeck@bwk.kuleuven.ac.be) (G. De Roeck).

theoretical analysis and numerical simulations [1]. This is to ensure the safety of bridge structures and the running stability of high-speed trains. Many useful results have been achieved from these studies. However, since there is not yet any high-speed railway line in operation for the moment now in China, these theoretical results need be supported and proved by experimental data. For this purpose, the Northern Jiaotong University in China, and the Catholic University of Leuven, the Free University of Brussels and the Belgium Railway Company SNCB in Belgium co-performed a project of field tests on high-speed railway bridge [2].

## 2. Experiment on Antoing Bridge

### 2.1. Introduction to the bridge

The Antoing Bridge is a railway bridge for the high-speed train Thalys between Paris and Brussels. The bridge is situated close to the Belgian–French border. The total bridge consists of successively five prestressed concrete (PC) bridges, a mixed steel–concrete bowstring bridge, which is built over a river, and a last 50 m span concrete bridge, see Fig. 1.

The PC bridges are simply supported girders with 50 m span and U-shaped cross-section, which are the main type of spans on the high-speed railway bridges in Belgium. The cross-section and the main dimensions of the girder are shown in Figs. 2 and 3, respectively.

### 2.2. Experimental arrangement

The experiment consists of two parts: the natural vibration property measurement and the dynamic response measurement of a 50 m U-section PC girder.

The vibration property measurement is focused on the bridge response to ambient vibration, from which the vibration properties such as the natural frequencies, mode shapes and damping ratios can be obtained. The excitation of the bridge is due to train passages primarily and to wind load, road traffic (underneath bridge) and micro-tremors.

The dynamic response measurement is to obtain the accelerations, strains and deflections of the bridge. The excitation is the high-speed Thalys train running through the bridge.



Fig. 1. View of Antoing Bridge.

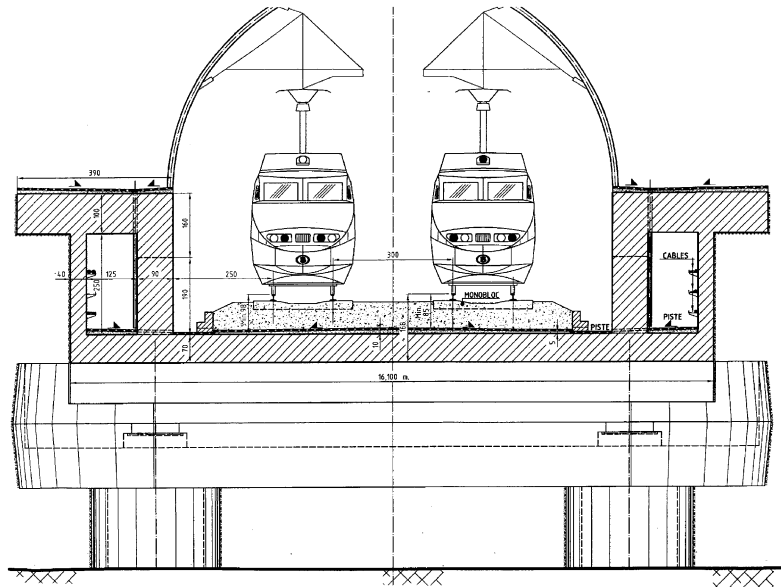


Fig. 2. Cross-section.

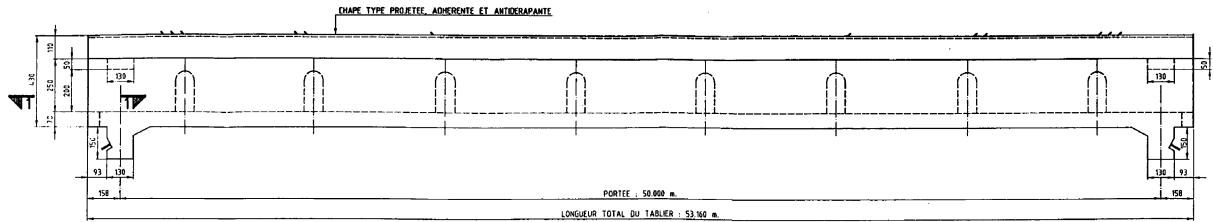


Fig. 3. Dimension of the 50 m U-section PC girder.

The sensor locations are indicated in Fig. 4. Each sensor location was given a unique number: *A* denotes acceleration measurement, *S* strain gauge measurement and *D* deflection measurement. Measurement direction is indicated by *x*, *y* or *z* (*x* longitudinal, *y* transverse, *z* vertical), respectively. Three reference accelerometers are used (*A3z*, *A4z*, *A4y*).

The bridge span is divided into 12 equidistant zones. A total of 29 vertical, 4 transversal and 2 longitudinal accelerations, 18 strains and 1 vertical deflection are measured.

At the lower side of the girder, at the mid-section, two rosettes of resistance strain gauges are glued, at the center and at the location under one of the railway tracks, to investigate the strain changes during train passages. At the same location of one of the strain rosettes, the vertical deflection at one point of the bridge girder is measured with a laser velocity displacement transducer (LVDT) mounted on a stiff, cable stayed pylon, see Fig. 5. Also at the same location, the acceleration is measured.

Measurement acquisition hardware equipment (portable PC, KEMO anti-aliasing filter and amplifier, DAT recorder) is installed at the transverse maintenance tunnel between the first and second span.

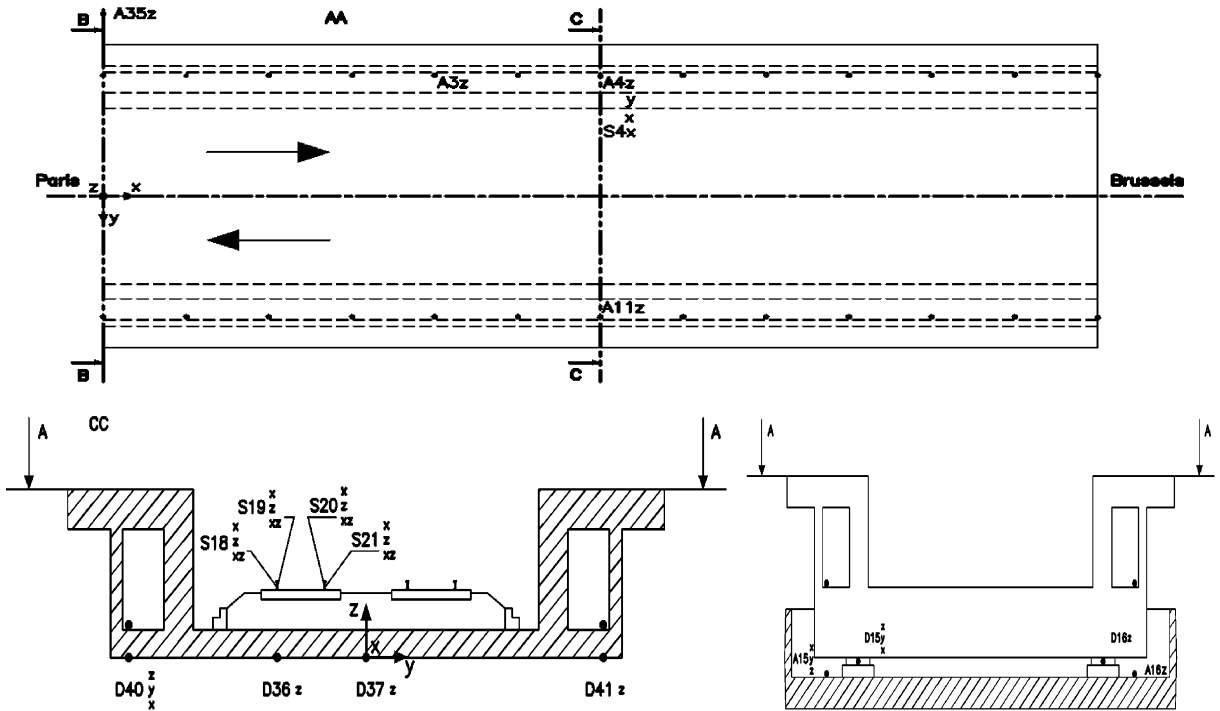


Fig. 4. Sensor locations in the experiment.



Fig. 5. Installation of LVDT and strain gauges.

To study the rigid body movement and relative movement of the girder with respect to the piers, the relative displacement at the neoprene bearing was measured ( $D15_{xyz}$  and  $D16z$ ) as well as the absolute acceleration at the pier top ( $A15_{xyz}$ ). Besides reference accelerations also one soil acceleration just besides a pier was included in the measurements.

For each set-up, three train passages are measured during 49 s; reference  $A3z$  is used as a trigger, with pre-trigger of 6 s. The cut-off frequency of the KEMO-filter is 100 Hz. For modal



Fig. 6. Thalys high-speed train on the bridge.

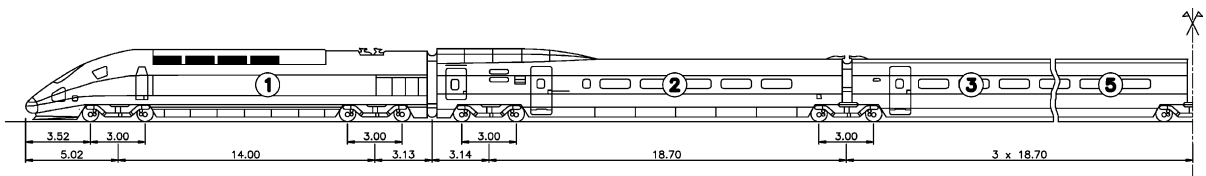


Fig. 7. High-speed Thalys train composition.

identification of the bridge, a digital resampling is applied to the measured accelerations, keeping finally the frequency interval up to 40 Hz. Fig. 6 shows the Thalys train running on the test bridge during the experiment.

### 2.3. Train properties

A single Thalys train is composed of a locomotive followed by a transition carriage, 6 normal carriages, a transition carriage and a locomotive, with 13 bogies in total. Fig. 7 shows the first three vehicles of the Thalys train. Table 1 lists the wheel positions, axle loads and the unsprung masses of a half single Thalys train.

### 2.4. Track properties

There is no direct data about the stiffness and damping features of the ballast. The rail pads have a static stiffness of 120 kN/mm in the load interval between 15 and 90 kN. Their dynamic stiffness is about 250 kN/mm for frequencies lower than 5 Hz. The rails are UIC60 profiles:  $A = 0.785 \times 10^{-2} \text{ m}^2$ ,  $I = 0.310 \times 10^{-4} \text{ m}^4$ . As sleepers, concrete bi-blocks are used.

The rail geometry and irregularities are measured, about every 5 months. Based on the interpretation of such a report, it could be concluded that, in the range of wavelengths from 1 to

Table 1  
Axle loads and unsprung masses

Axle number	Position (mm)	Load (kN)	Unsprung mass (kg)
1	0	166.6	1732
2	3000	166.6	1732
3	14,000	166.6	1732
4	17,000	166.6	1732
5	20,267	142.1	1826
6	23,267	142.1	1826
7	38,967	142.1	1826
8	41,967	166.6	1830
9	57,667	166.6	1830
10	60,667	166.6	1830
11	76,367	166.6	1830
12	79,367	166.6	1830
13	95,067	166.6	1830

31.5 cm, the rail quality can be classified as very good, following the criteria given by Braun and Hellenbroich [3].

To control the overall comfort quality of the high-speed track, a measurement carriage, equipped with accelerometers on the vehicle body and on the bogies, is coupled to a normal Thalys train, called ‘Melusine’, running at a constant speed of 300 km/h.

### 3. Experimental results

#### 3.1. Modal parameters

The stochastic subspace identification technique is used to extract the modal characteristics from the data [4]. The technique has been implemented (SPICE [5]) in the MATLAB environment [6]. Treatment of the free vibration data after train passage results in the frequencies and the damping ratios of Table 2, in which the modal results from the tuned FE model are also provided for comparison.

The characterization of the modes follows from inspection of the FE results. It is confirmed by the experimental results (Fig. 8), although the visualization might be incomplete because only two measurement lines are considered on either side of the bridge (Fig. 4).

Because of the two symmetry planes of the bridge the modes should possess symmetry or antisymmetry with regard to these two planes. This is approximately fulfilled (Fig. 8): symmetric (longitudinal)–symmetric (transversal) (modes 1, 3, 6), symmetric (longitudinal)–antisymmetric (transversal) (mode 2), antisymmetric (longitudinal)–symmetric (transversal) (mode 4), antisymmetric (longitudinal)–antisymmetric (transversal) (mode 5).

Fig. 8 shows also that the supports (neoprene bearings on columns) cannot be considered as infinitely stiff.

Table 2  
Theoretical and experimental modal characteristics

Mode	Eigenfrequency (Hz)		Damping ratio (%)	Characterization of mode
	Theoretical	Experimental		
B1	3.19	3.19	0.63	First bending (symmetric)
T1	3.95	3.87	2.98	First torsional (symmetric)
S1	6.70	6.84	2.74	First bending of cross-section (symmetric)
B2	9.20	8.77	2.24	First antisymmetric bending
T2	10.39	10.56	1.83	Second torsional (antisymmetric)
S2	12.33	12.46	1.52	Second bending of cross section (antisymmetric)
B3	14.57	18.56	1.52	Second symmetric bending
B4	18.44	19.28	1.56	Second antisymmetric bending

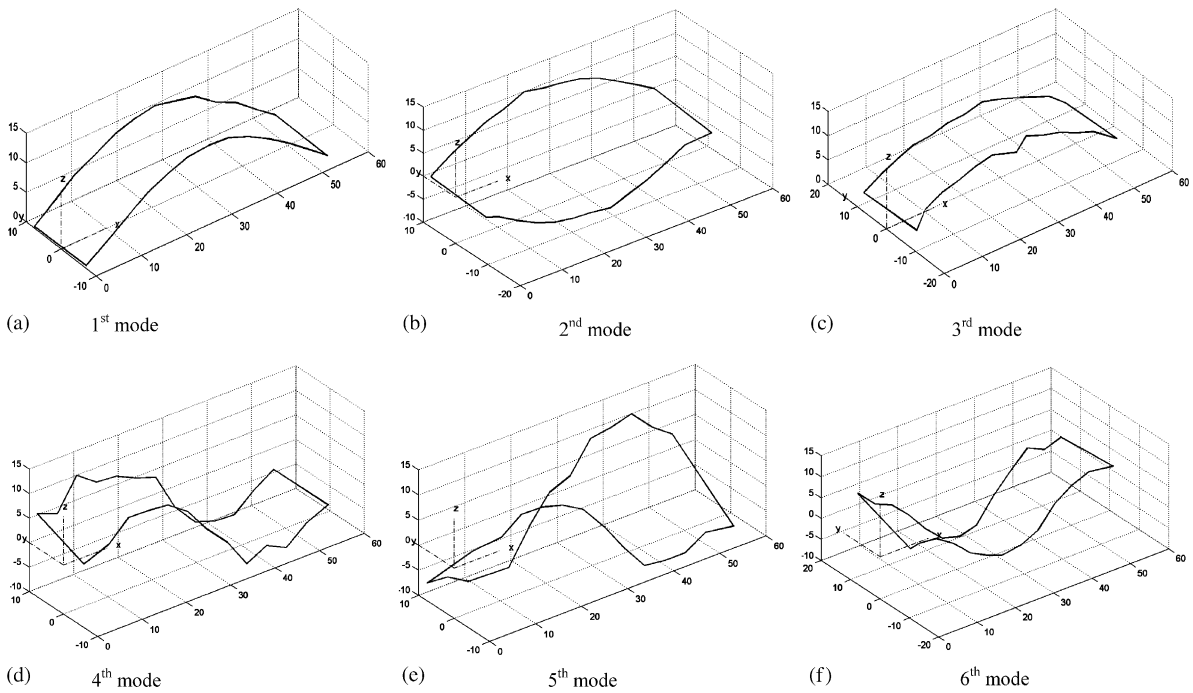


Fig. 8. Experimental bridge modes.

### 3.2. Dynamic responses

In the experiment, there are in total 19 measurements which have been recorded and analyzed. The speed of the Thalys train running through the bridge was 260–310 km/h. In the figures and the following statements, the trains are marked as T for single Thalys composition and 2T for double Thalys composition, respectively. Some of the results are given below.

In Ref. [7] it is shown that the dynamic responses can be accurately predicted by an FE-model with running point loads.

### 3.2.1. Vertical deflection

The vertical deflection measured by the LVDT on the stiff antenna, at the center of the span of the girder under single Thalys and double Thalys trains are shown in Fig. 9. The distribution of the bridge deflection versus the train speed is shown in Fig. 10.

The results show that the deflections of the girder under the single Thalys and the double Thalys running on the passage side of the measurement are 1.6 and 1.75 mm, respectively. When the trains run on the second track of the bridge, the deflection is measured as 0.7 mm for single Thalys and 0.85 mm for double Thalys. It can be deduced that the deflection at the central line of the girder is about 1.3 mm, thus the corresponding rotational movement is about  $(1.6-0.85)/4500 = 1/6000$  or  $(1.75-0.85)/4500 = 1/5000$ , where 4500 mm is the center-to-center distance between the two tracks.

According to the influence line loading of the axle load by FE-calculations, the static deflections of the girder under single and double Thalys are 1.28 and 1.45 mm. The experimentally derived impact factors can therefore be estimated as  $1.6/1.28 = 1.25$  for a single Thalys and  $1.75/1.45 = 1.21$  for a double Thalys, respectively.

### 3.2.2. Vertical acceleration

The typical vertical acceleration curves under single and double Thalys trains are shown in Fig. 11. The vertical accelerations of each passage measured by the accelerometers on the girder, at the mid-span of the girder under Thalys trains running on the passage side and the second track of the bridge are plotted in Fig. 12.

The maximum vertical ( $z$ -) acceleration of the bridge is about  $0.76 \text{ m/s}^2$ . This result is somewhat dependent on the set acquisition parameters. The maximum difference of the accelerations at the passage side and the second track is  $0.37 \text{ mm/s}^2$ . There is no obvious difference between the vertical accelerations induced by single Thalys and double Thalys trains.

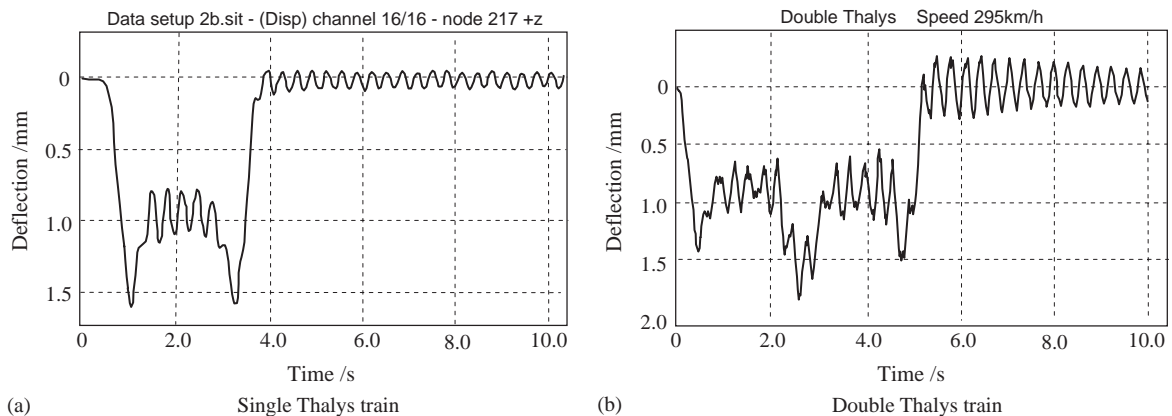


Fig. 9. Deflection curve of the girder at mid-span.



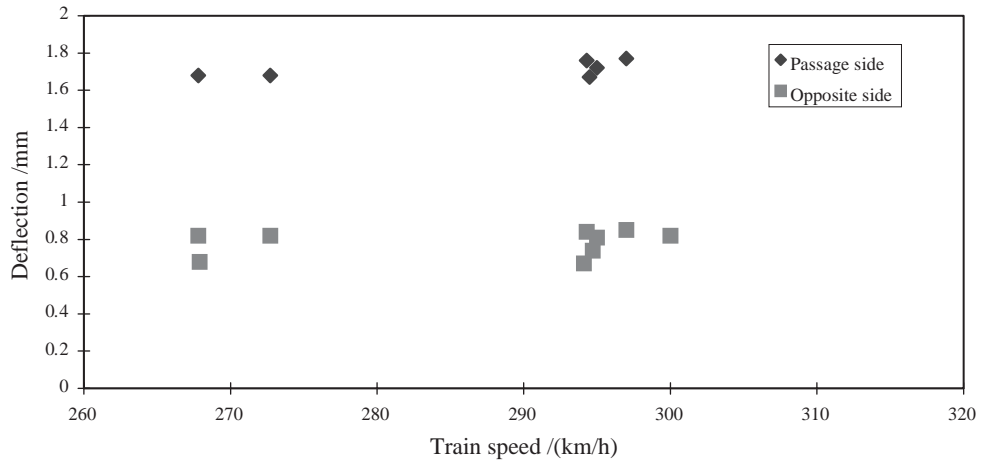


Fig. 10. Distribution of bridge deflection versus train speed.

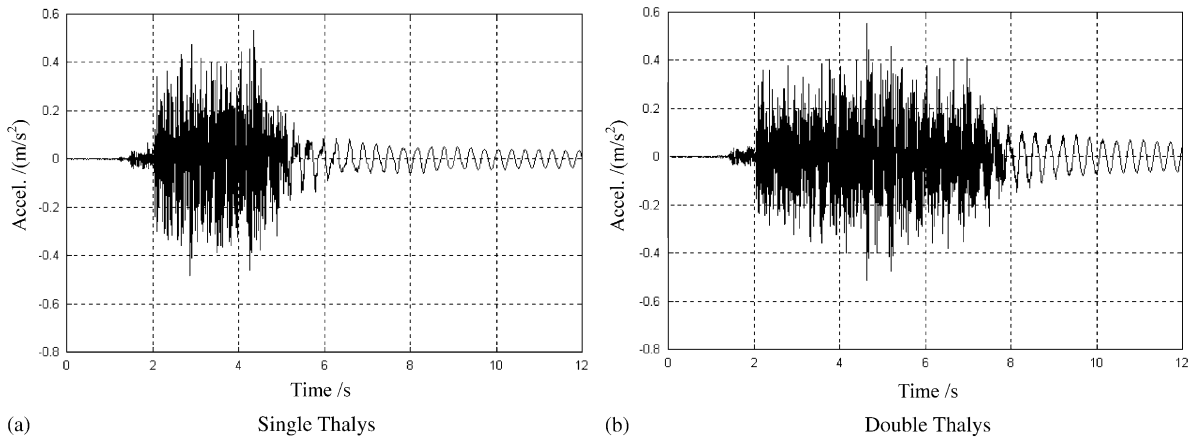


Fig. 11. Vertical acceleration curve of the girder.

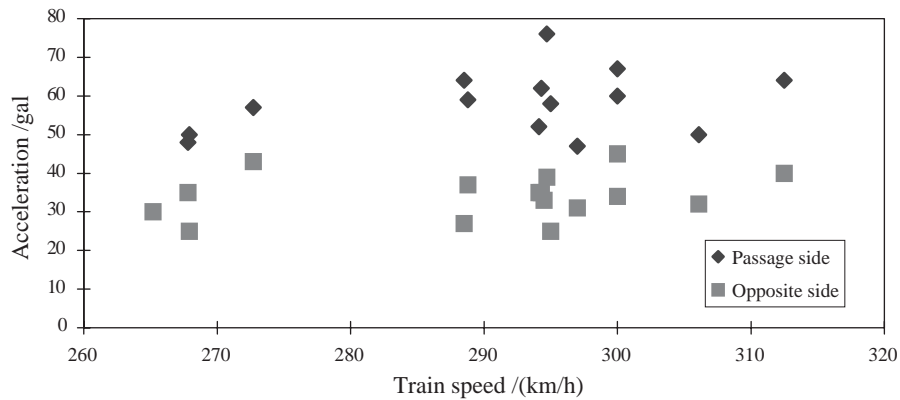


Fig. 12. Distribution of bridge vertical acceleration versus train speed.

3.2.3. Lateral acceleration

The typical lateral acceleration curves under single and double Thalys trains are shown in Fig. 13. The lateral accelerations of each passage measured by the accelerometers on the girder, at the mid-span of the girder and the pier top are plotted in Fig. 14. The lateral ( $y$ -) accelerations of the bridge are very small. The maximum acceleration is  $0.174 \text{ m/s}^2$  under double Thalys train. The measured lateral accelerations at the pier top are ranged between  $0.017 \text{ m/s}^2$  and  $0.138 \text{ m/s}^2$ , with the average  $0.085 \text{ m/s}^2$  and standard variation  $0.042 \text{ m/s}^2$ . The results show that the lateral vibrations of the bridge are very small and there is no obvious difference between the lateral accelerations induced by single Thalys and double Thalys trains.

3.2.4. Strain of girder concrete

The strain gauge signals ( $S17x$ ) under single and double Thalys trains are denoted in Fig. 15. Although the strain level reaches a low peak value of  $10 \mu\text{S}$ , the 13 bogie passages are clearly detectable. Bogies 2, 3 and 11, 12 are close resulting in double peak in the time signal. From this time signal the train speed is estimated at  $265 \text{ km/h}$ .

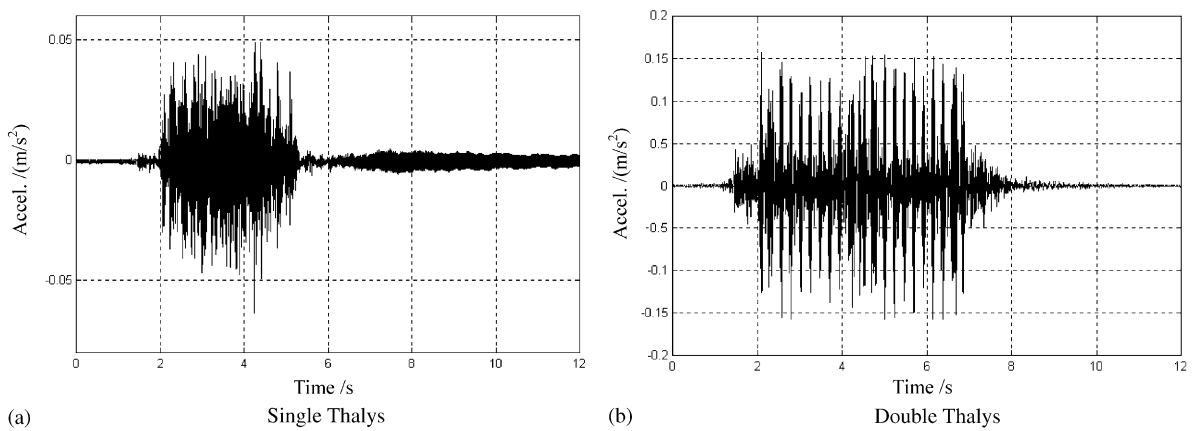


Fig. 13. Lateral acceleration curve of the girder.

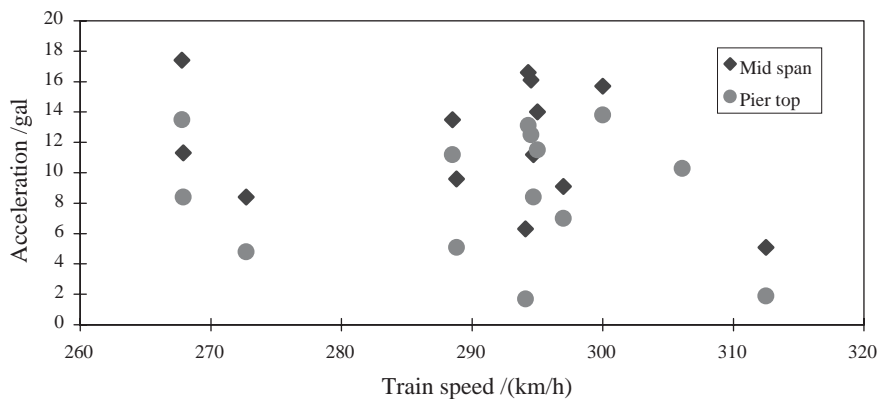


Fig. 14. Distribution of lateral accelerations of bridge span and pier top versus train speed.

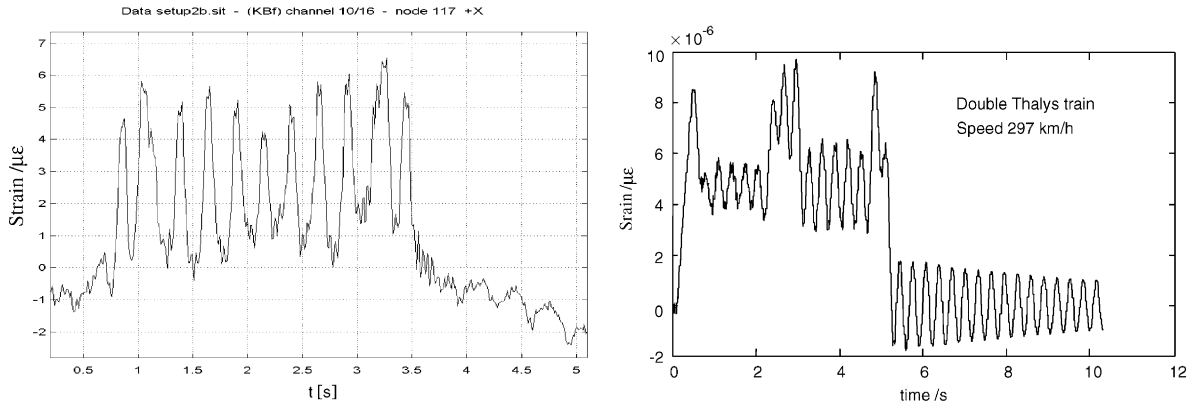


Fig. 15. Measured strain curve.

### Acknowledgements

This study is sponsored by the Bilateral Research Project (BIL98/09) from the Ministry of the Flemish Community of Belgium and the National Natural Science Foundation of China (No. 50078001).

### References

- [1] Xia He, Dynamic Interaction Between Vehicles and Structures, Science Press, Beijing, 2002, pp. 143–149.
- [2] Maeck J, Teughels A, De Roeck G, Experimental and numerical modal analysis of a concrete high speed train railway bridge, in: Xia He (Ed.), Proceedings of the MCCI'2000, Vol II, Delft University Press, Delft, 2000, pp. 61–68.
- [3] H. Braun, T. Hellenbroich, Meßergebnisse von Straßenunebenheiten, VDI Berichte 877 (1991) 47–80.
- [4] ANSYS Version 5.6, ANSYS Inc., Canonsburg, PA, USA.
- [5] B. Peeters, G. De Roeck, Reference based stochastic subspace identification in civil engineering, Inverse Problems in Engineering 8 (1) (2000) 47–74.
- [6] B. Peeters, B. Van den Branden, G. De Roeck, Output-only modal analysis: a GUI for MATLAB, 2nd Benelux Matlab Users Conference, Brussels, Belgium, 1999.
- [7] G. De Roeck, A. Maeck, A. Teughels, Train–bridge interaction validation of numerical models by experiments on high-speed railway bridge in antoing, Proceedings of the TIVC'2001, Beijing, pp. 283–294.